Article

Cell Reports

Loss of Survivin in Intestinal Epithelial Progenitor Cells Leads to Mitotic Catastrophe and Breakdown of Gut Immune Homeostasis

Graphical Abstract

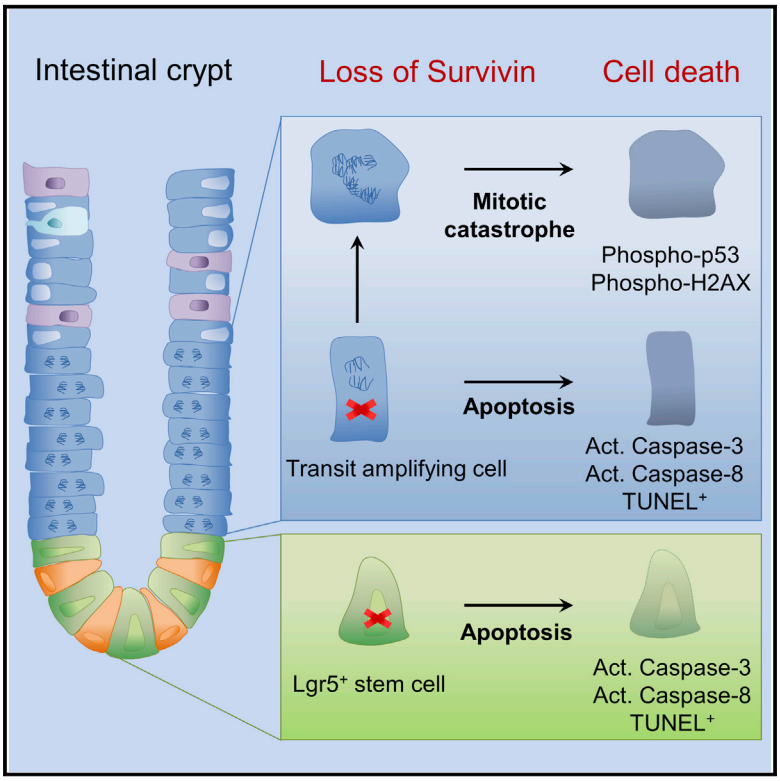

Highlights

- Survivin is expressed in stem and progenitor cells of the intestinal epithelium
- Deletion of Survivin in IECs leads to death of animals within a few days
- Survivin deletion induces loss of transit-amplifying cells and Lgr5$^+$ stem cells
- Survivin-deficient cells show cell-cycle defects and signs of mitotic catastrophe

Authors

Eva Martini, Nadine Wittkopf, Claudia Günther, ..., Kerstin Amann, Markus F. Neurath, Christoph Becker

Correspondence

christoph.becker@uk-erlangen.de

In Brief

Martini et al. discover an essential role of the IAP protein family member Survivin in the maintenance of tissue homeostasis in the gut. They show that Survivin-deficient epithelial stem and progenitor cells succumb to mitotic catastrophe, leading to secondary inflammation.

Martini et al., 2016, Cell Reports *14*, 1062–1073
February 9, 2016
http://dx.doi.org/10.1016/j.celrep.2016.01.010

CellPress

OPEN ACCESS
CellPress

Cell Reports
Article

Loss of Survivin in Intestinal Epithelial Progenitor Cells Leads to Mitotic Catastrophe and Breakdown of Gut Immune Homeostasis

Eva Martini,[1] Nadine Wittkopf,[1] Claudia Günther,[1] Moritz Leppkes,[1] Hitoshi Okada,[2] Alastair J. Watson,[3] Eva Podstawa,[1] Ingo Backert,[1] Kerstin Amann,[4] Markus F. Neurath,[1] and Christoph Becker[1,*]
[1]Department of Medicine 1, University Medical Center, Friedrich-Alexander-University, 91052 Erlangen, Germany
[2]Department of Biochemistry, Kindai University Faculty of Medicine, Osaka 589-8511, Japan
[3]Norwich Medical School, University of East Anglia, Norwich Research Park, Norwich, Norfolk NR4 7TJ, UK
[4]Department of Nephropathology, University Medical Center, Friedrich-Alexander-University, 91052 Erlangen, Germany
*Correspondence: christoph.becker@uk-erlangen.de
http://dx.doi.org/10.1016/j.celrep.2016.01.010

SUMMARY

A tightly regulated balance of proliferation and cell death of intestinal epithelial cells (IECs) is essential for maintenance of gut homeostasis. Survivin is highly expressed during embryogenesis and in several cancer types, but little is known about its role in adult gut tissue. Here, we show that Survivin is specifically expressed in transit-amplifying cells and Lgr5$^+$ stem cells. Genetic loss of *Survivin* in IECs resulted in destruction of intestinal integrity, mucosal inflammation, and death of the animals. Survivin deletion was associated with decreased epithelial proliferation due to defective chromosomal segregation. Moreover, *Survivin*-deficient animals showed induced phosphorylation of p53 and H2AX and increased levels of cell-intrinsic apoptosis in IECs. Consequently, induced deletion of *Survivin* in Lgr5$^+$ stem cells led to cell death. In summary, Survivin is a key regulator of gut tissue integrity by regulating epithelial homeostasis in the stem cell niche.

INTRODUCTION

The intestinal epithelium is a vigorously self-renewing tissue where stem cells and transit-amplifying (TA) cells at the base of the crypts give rise to terminally differentiated cells. In the small intestine, these cells migrate up toward the villous tip, from where they are shed into the lumen to be replaced by neighboring cells (Sancho et al., 2003). Since the epithelium acts as a barrier against a plethora of antigens in the intestinal lumen, the balance between proliferation and cell death must be tightly regulated to maintain homeostasis in the intestinal tract. Accordingly, an overproduction of intestinal epithelial cells (IECs) can lead to the development of tumors, whereas excessive death of IECs can cause breakdown of the intestinal barrier and may lead to invasion of bacteria. The intestinal stem cell niche is built of stem cells intermingled with Paneth cells located at the 0 to +4 position and TA cells, located above the +4 position (Barker et al., 2012). Intestinal stem cells are characterized by the expression of distinct genes, for instance the leucine-rich repeat-containing G-protein-coupled receptor 5 (*Lgr5*), B lymphoma Mo-MLV insertion region 1 homolog (*Bmi1*), and Olfactomedin 4 (*Olfm4*) (Barker et al., 2010). TA cells are fast-cycling progeny of stem cells and important for replacement of shed epithelial cells (Barker et al., 2012).

Survivin is a member of the inhibitors of apoptosis (IAP) protein family and expressed during embryonic development. Embryos with homozygous general deletion of *Survivin* failed to survive beyond embryonic day 4.5 (E4.5) (Uren et al., 2000), whereas heterozygous deletion of the *Survivin* gene allowed normal development, although embryos were more sensitive to Fas-mediated hepatic apoptosis (Conway et al., 2002). In contrast to its well-described function in embryonic development, the role of Survivin in adult tissue remains unclear, as differentiated cells show almost no Survivin expression (Fukuda and Pelus, 2006). The role of Survivin seems to be highly tissue dependent, as deficiency for *Survivin* in pancreas and liver showed no severe effect on tissue homeostasis, while deficiency in the brain and heart led to premature death of the animals (Jiang et al., 2005; Levkau et al., 2008). On the molecular level, Survivin is linked to several cellular circuitries including the inhibition of apoptosis, stress responses, angiogenesis, and the p53 checkpoint, depending on the cellular context and the tissue (Altieri, 2006). Several of these functions are key regulators of cellular homeostasis and involved in tumor development. Importantly, Survivin is highly expressed in several cancer types, including colorectal cancer (Fukuda and Pelus, 2006). As a consequence of this cancer-cell-specific overexpression of Survivin, considerable efforts have been made to target Survivin for cancer therapy by the use of antagonizing agents or immunotherapies (Mobahat et al., 2014). Moreover, Survivin appears to be a reliable diagnostic marker to predict colorectal cancers (Miura et al., 2011), and high Survivin levels are associated with poor overall survival (Huang et al., 2013). Despite the important role of Survivin in several tissues, the function of Survivin in the gut is currently unknown. Using conditional knockout mice allowing control of

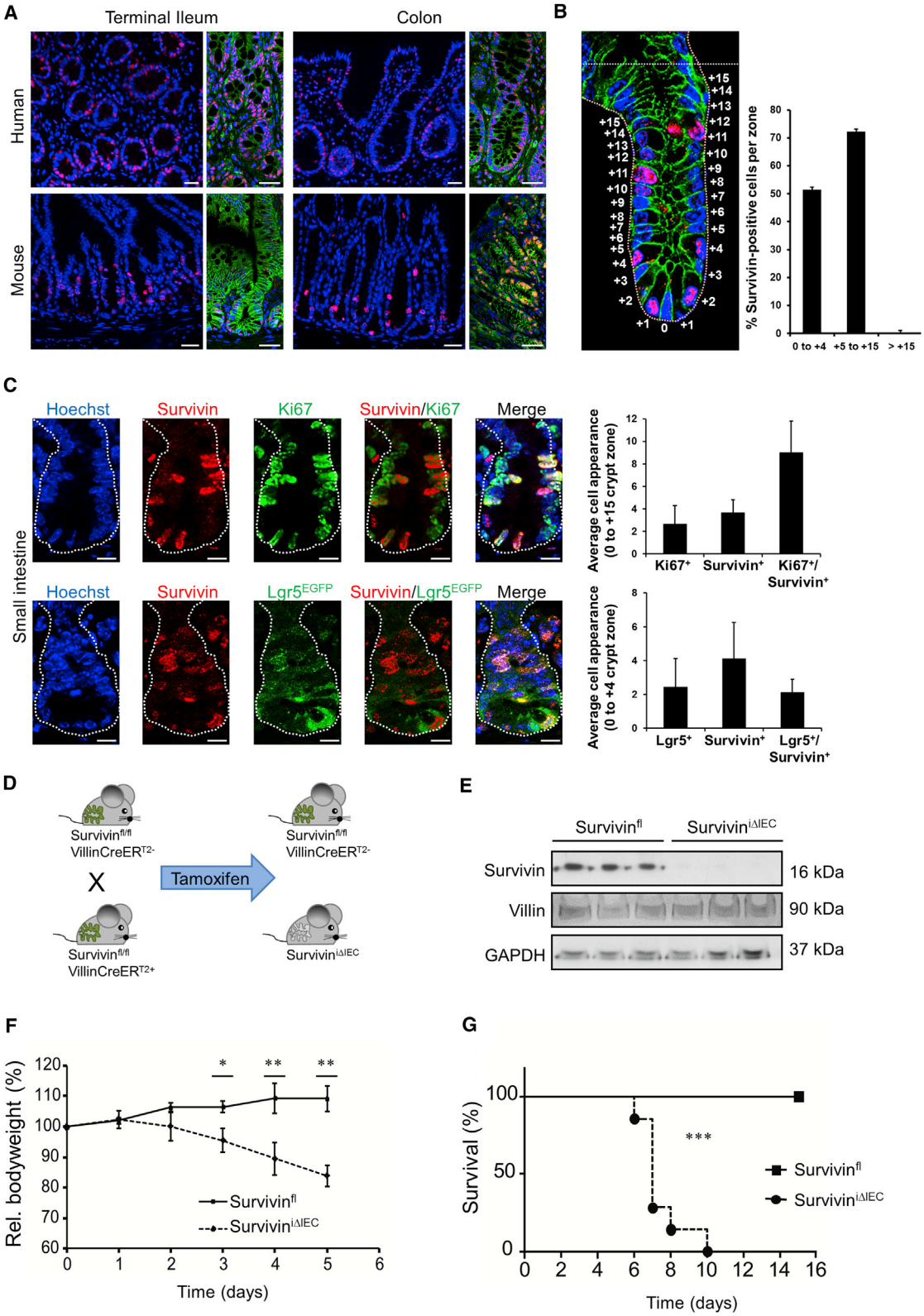

(legend on next page)

Survivin expression in a temporal and tissue-specific manner, we here demonstrate a crucial importance for Survivin expression in epithelial progenitor cells for gut development as well as immune and tissue homeostasis.

RESULTS

Deletion of *Survivin* in the Intestinal Epithelium Leads to Severe Destruction of Gut Morphology

Survivin is known to be highly expressed during embryonic development. To investigate whether Survivin might also be expressed in the adult intestinal epithelium, we initially analyzed Survivin in the gut of mice and humans under physiologic conditions. In agreement with previously published data (Boman et al., 2009; van de Wetering et al., 2002), we observed expression of Survivin in healthy gut samples of adult mice and humans. Survivin expression was restricted to the intestinal epithelium of the crypt compartment of the small and large intestine of both mice and humans (Figures 1A and S1A). Detailed analysis of Survivin expression within the crypts of the small intestine of mice showed positivity of almost 50% of total cells in the stem cell niche at the bottom of the crypt (0 to +4) and positivity of more than 70% of total cells in the TA cell area (+5 to +15). No Survivin expression was found outside of the crypts (>+15; Figure 1B). To further narrow down which cell types in the crypt compartment expressed Survivin, we simultaneously stained for Survivin and specific cell markers. We observed expression of Survivin in half of the Lgr5-positive cells and in two-thirds of Ki67 positive cells (Figures 1C and S1B), suggesting that the protein is expressed in stem cells at the crypt base and in mitotic cells of the TA cell area. In support of this conclusion, we could show increased Survivin expression in the G2/M phase of cell-cycle-sorted IECs (Figure S1C). To further investigate whether Survivin in IECs is important for gut homeostasis in adult mice, we crossbred Survivin$^{fl/fl}$ mice to mice carrying the inducible CreER^{T2} recombinase under the control of the Villin promotor (Villin-CreER^{T2}). To induce the *Survivin* knockout in IECs in adult mice (Survivin$^{i\Delta IEC}$) and investigate the role of Survivin in the mouse intestine, we treated 6- to 12-week-old mice with a daily injection of 1 mg tamoxifen (Figure 1D). Knockout of the *Survivin* gene was confirmed by allele-specific PCR (Figure S1D) and the loss of the protein by western blot analysis of isolated intestinal epithelial cells (Figure 1E). Remarkably, mice immediately started losing weight following *Survivin* deletion in adult mice (Figure 1F), and all animals died within 6 to 10 days (Figure 1G). Compared to control littermates, Survivin$^{i\Delta IEC}$ mice showed significantly reduced gut length (Figure 2A). Moreover, high-resolution video endoscopy indicated massive destruction of the villous structure in the small intestine and colon of Survivin$^{i\Delta IEC}$ mice compared to control mice (Figure 2B). Additional microscopic analysis (Figure 2C, left) and histological scoring (Figure 2C, right) revealed epithelial erosions, loss of the regular crypt-villus architecture, and overall severe tissue destruction of the small intestine and colon in Survivin$^{i\Delta IEC}$ mice compared to controls. Consequently, we found infiltration of neutrophils after 96 hr following induction of *Survivin* deletion, shown by the expression of myeloperoxidase (Figure S1E). Moreover mRNA expression of tumor necrosis factor alpha (*TNF-*α) was also highly upregulated in Survivin$^{i\Delta IEC}$ mice 96 hr after Survivin deletion correlating with an infiltration of neutrophils (Figure S1F).

In summary, our data demonstrate the essential function for Survivin for embryonic development as well as for adult tissue homeostasis in the gut. Loss of Survivin leads to irreparable tissue damage followed by severe immune responses.

Survivin Is Essential for Maintenance of the Transit-Amplifying and Stem Cell Niche

Loss of Survivin in IECs led to a dramatic phenotype that was affected by destruction of complete gut architecture, indicating a disturbance in epithelial cell homeostasis. As mentioned above, Survivin expression is restricted to the crypt. In agreement with the severe phenotype observed after tamoxifen injection, Survivin expression in the lower crypt compartment of small intestine and colon of Survivin$^{i\Delta IEC}$ mice was almost completely diminished (Figures 3A and S1G). The reduction of Survivin had only little influence on the expression of differentiated epithelial cell types shown by the expression of specific genes (Figure S2A, top). All differentiated epithelial cell types could be found in control and Survivin$^{i\Delta IEC}$ mice, shown by staining of specific cell types. Goblet cells and Paneth cells showing signs of degranulation but are expressed in equal amounts (Figure S2A, bottom). In sharp contrast, the expression of stem cell related genes like *Ofm4* and *Lgr5* were significantly reduced after *Survivin* deletion (Figure 3B). We further investigated if this reduction of stem cell

Figure 1. Survivin Is Exclusively Expressed in the Intestinal Crypt Compartment and Essential for Survival

(A) Expression of Survivin (red) in mouse and human terminal ileum as well as colon tissue. High-power views show Survivin expression (red) together with E-cadherin (green). Scale bars, 25 μm. Nuclei were counterstained with Hoechst 33342 (blue).

(B) Left: representative staining for Survivin (red) and E-cadherin (green) of a small intestinal crypt. Nuclei were counterstained with Hoechst 33342 (blue). Cells of the crypt were sectioned into the lower crypt zone (0 to +4), the upper crypt zone (+5 to +15) and non-crypt zone (> +15). Right: graph represents the percentage of Survivin-positive cells per crypt zone ($n \geq 6$ crypts per group). Data represent mean values ± SD.

(C) Representative confocal microscopy pictures of small intestine of Survivin^{fl} mice stained for Survivin (red) and Ki67 (green) (top) as well as Survivin (red) and EGFP in Lgr5^{EGFP} mice (green) (bottom). Nuclei were counterstained with Hoechst 33342 (blue). Scale bars, 10 μm. Graphs represent the average appearance of single-positive cells (Survivin, Ki67, and Lgr5) as well as double-positive cells (Survivin/Ki67 and Survivin/Lgr5) in the crypt. Data represent mean values ± SD.

(D) Survivin$^{fl/fl}$ Villin-CreER^{T2-} mice and Survivin$^{fl/fl}$ Villin-CreER^{T2+} mice were used to analyze Survivin deletion in the intestine. Mice were injected with tamoxifen (final concentration 1 mg) to induce Survivin deletion specifically in IECs (Survivin$^{i\Delta IEC}$).

(E) Western blot analysis shows reduced Survivin level in IECs of Survivin$^{i\Delta IEC}$ mice after 4 days of tamoxifen treatment. Internal controls: Villin and GAPDH.

(F) Relative weight of control and Survivin$^{i\Delta IEC}$ mice during tamoxifen treatment was monitored over time and is indicated as percent (%) of the initial weight ± SD ($n = 3$ mice per group). Experiment was repeated three times with similar results.

(G) Kaplan-Meier survival curve showing survival of control and Survivin$^{i\Delta IEC}$ mice after a daily injection of tamoxifen ($n = 7$ mice per group).

See also Figure S1.

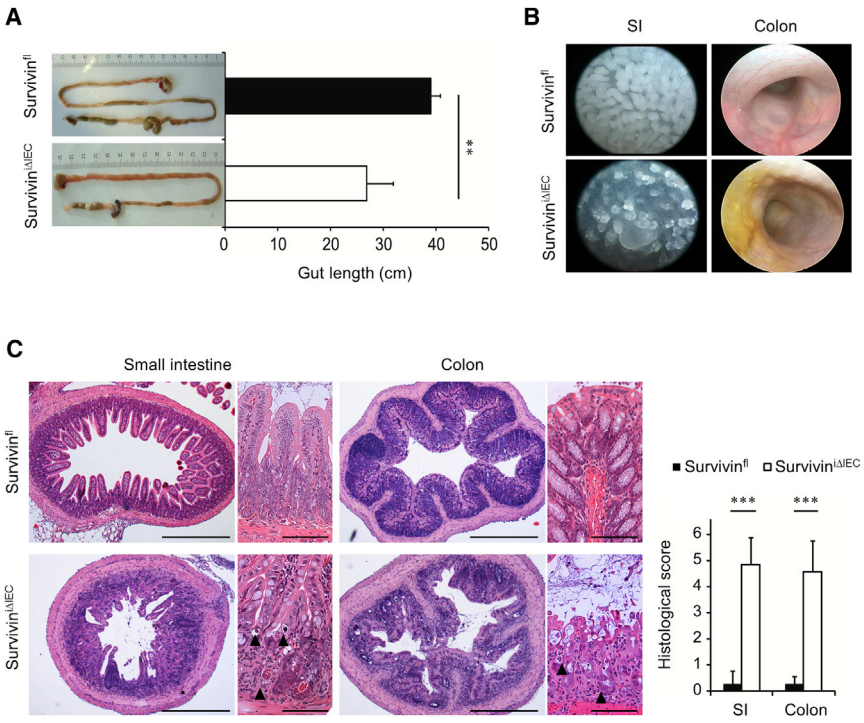

Figure 2. Deletion of Survivin in the Intestinal Epithelium Leads to Disruption of Intestinal Tissue Homeostasis

(A) Representative pictures of the intestine of control and Survivin$^{i\Delta IEC}$ mice treated for 4 days with tamoxifen and statistical analysis of the gut length (n = 4 mice per group). Data represent mean values + SD.

(B) Representative endoscopic pictures of the small intestine (SI) and the colon of control and Survivin$^{i\Delta IEC}$ mice 6 days after tamoxifen treatment.

(C) Left: histological H&E stainings of small intestine and colon of control and Survivin$^{i\Delta IEC}$ mice. Scale bars, 500 μm; inset, 100 μm. Right: histological scoring evaluating tissue destruction and epithelial erosions of small intestine (SI) and colon from Survivin$^{i\Delta IEC}$ and control mice 5 days after tamoxifen injection. Data represent mean values + SD ($n \geq 6$ mice per group). Arrows indicate intestinal epithelial erosions.

See also Figure S1.

marker genes leads to a proliferation defect in IECs and pulse-labeled IECs in vivo with bromodeoxyuridine (BrdU), which revealed greatly reduced proliferation within 48 hr after tamoxifen injection in Survivin$^{i\Delta IEC}$ mice (Figure 3C). This was confirmed by demonstrating reduced expression of Ki67 when Survivin was deleted (Figure S2B). Therefore, our data indicate that Survivin depletion leads to dysregulations in the epithelial turnover.

We next investigated whether excessive cell death might be the cause for rapid tissue destruction after deletion of Survivin. Mice were treated with tamoxifen for the duration of 96 hr, and tissue was analyzed every 24 hr. We detected significantly increased apoptosis, marked by elevated numbers of TUNEL and activated caspase-3-positive cells in Survivin$^{i\Delta IEC}$ mice at the crypt bottom already after 24 to 48 hr (Figure 4A). Interestingly, double staining for Ki67 and TUNEL in Survivin$^{i\Delta IEC}$ mice showed pronounced cell death in proliferating cells within the crypt in an area where TA cells and stem cells reside (Figure 4B). This could be confirmed by western blot analysis showing increased levels of activated caspase-3 and caspase-8 (Figure 4C). Cell death following Survivin deletion was further detected in in vitro generated organoids of Survivin$^{i\Delta IEC}$ mice after stimulation with tamoxifen for 4 days (Figures 4D and S2C), suggesting that cell death was induced by a cell-intrinsic mechanism rather than death receptor signaling. This conclusion was further supported by crossing inducible *Survivin* deficient mice on a *Caspase-8* deficient (Casp8/Survivin$^{i\Delta IEC}$) or a *RIPK3* deficient (RIPK3/Survivin$^{i\Delta IEC}$) background to evaluate whether either excessive extrinsic apoptosis or necroptosis could explain the severe phenotype of Survivin$^{i\Delta IEC}$ mice. As indicated by histochemical analysis, neither genotype could rescue the lethal outcome of Survivin deletion (Figure S3A). Similarly, neither blocking of caspase-8, RIPK3, or a combination of both, nor blocking of TNF-α, prevented organoid death in vitro following deletion of Survivin, as indicated by propidium iodide (PI) staining and morphological disintegration (Figures S3B and S3C). In summary, our data support the view that loss of Survivin specifically induces cell death in cycling cells at the crypt bottom by a primary cell-intrinsic mechanism that affects the regenerative potential of the epithelium leading to severe gut pathology.

Since Lgr5-expressing stem cells at the crypt bottom are considered an essential source for intestinal epithelial regeneration, we crossed Lgr5-EGFP-IRES-CreER^{T2} mice to Survivin$^{fl/fl}$ mice (Lgr5$^{i\Delta Survivin}$) in order to directly analyze the effects of loss of Survivin in the stem cell niche. We could confirm the mosaic pattern of EGFP expression of the Lgr5-EGFP-IRES-CreER^{T2} construct in this mouse model (Barker et al., 2010). Importantly, Lgr5$^{i\Delta Survivin}$ mice showed a reduction of the EGFP signal in the small intestine as well as the colon after 5 days of tamoxifen treatment (Figure S4A). Furthermore, flow-cytometry-based analysis of isolated Lgr5-EGFP-expressing stem cells from mice injected with tamoxifen for 3 days indicated a reduction of EGFP expression (Figure 5A). To provide additional evidence for a role of Survivin in Lgr5 expressing stem cells, we generated organoids from control and Lgr5$^{i\Delta Survivin}$ mice in the presence of CHIR99021, an inhibitor of the glycogen synthase kinase 3 (GSK-3), and valproic acid, a histone deacetylase (HDAC) inhibitor, to expand the population of Lgr5-EGFP-expressing stem cells (Figure S4B). Combined treatment with CHIR99021 and valproic acid has been demonstrated to maintain self-renewal of mouse Lgr5^{+} intestinal stem cells (Yin et al., 2014). Lgr5$^{i\Delta Survivin}$ organoids treated for 3 days with tamoxifen showed increased levels of cell death as demonstrated by activated caspase-3 staining and a reduced expression of EGFP (Figures 5B–5D), indicating a loss of Lgr5 expressing cells. Activation of cell death programs in Lgr5-expressing cells was further confirmed

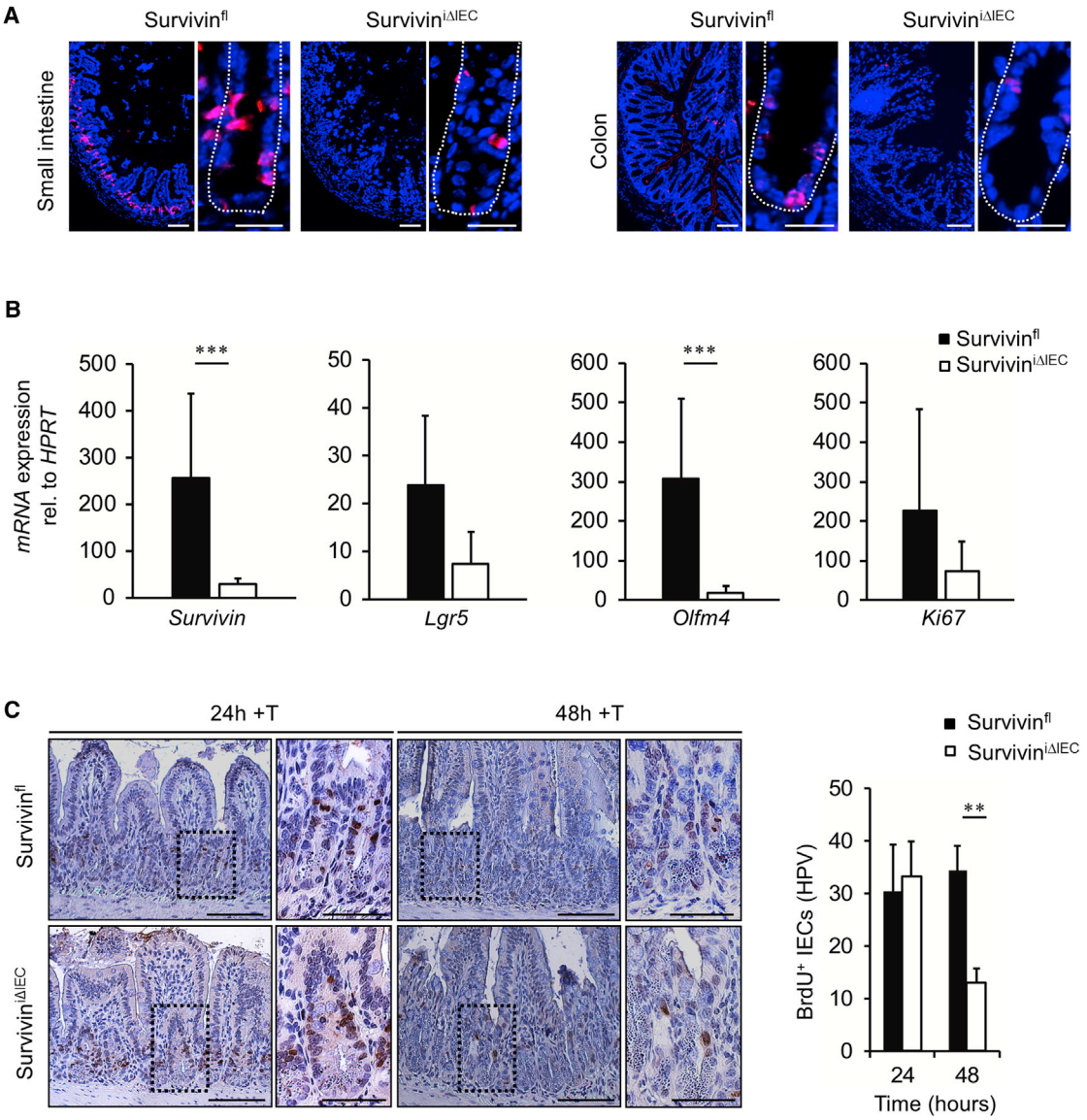

Figure 3. Loss of Survivin Leads to Cell Death in the Crypt Compartment

(A) Expression of Survivin (red) in small intestine and colon of Survivin$^{i\Delta IEC}$ and control mice after 6 days of tamoxifen treatment. Scale bars, 100 μm; insets, 25 μm.

(B) mRNA expression of *Survivin*, *Lgr5*, *Olfm4*, and *Ki67* in small intestinal tissue relative to *HPRT* from Survivin$^{i\Delta IEC}$ and control mice after 4 days of tamoxifen injection. Data represent mean values + SD (n ≥ 6 mice per group).

(C) BrdU staining (brown) in the small intestine of Survivin$^{i\Delta IEC}$ and control mice after 24 and 48 hr (h) tamoxifen (+T) treatment and pulse injection of BrdU. Nuclei were counterstained with hematoxylin (blue). BrdU positive ($^+$) intestinal epithelial cells (IECs) per high-power view (HPV) were counted for statistical analysis. Data represent mean values + SD (n = 3 mice per group). Scale bar, 100 μm; high-power view scale bar, 50 μm.

See also Figure S2.

by western blot analysis of isolated IECs indicating increased levels of activated caspase-3 and activated caspase-8 in Lgr5$^{i\Delta Survivin}$ mice 1 day after tamoxifen treatment (Figure 5E). Furthermore, we could detect significantly more activated caspase-3-positive cells in the crypt compartment of Lgr5$^{i\Delta Survivin}$ mice after treatment with tamoxifen for 1 day (Figure S4C). Taken together, our data demonstrated that Survivin is absolutely essential for maintaining stem and progenitor cell homeostasis and regeneration of the epithelium.

Loss of Survivin Leads to Abnormal Cell Division and Signs of Mitotic Catastrophe in the Intestinal Crypt Compartment

To gain further insight into triggering factors of progenitor cell death in the absence of Survivin, we further analyzed crypt cells using electron microscopy. Electron microscopy pictures showed loss of the crypt architecture in Survivin$^{i\Delta IEC}$ mice when compare to control mice. Specifically, we observed a loss of crypt base columnar cells, stem cells defined by their

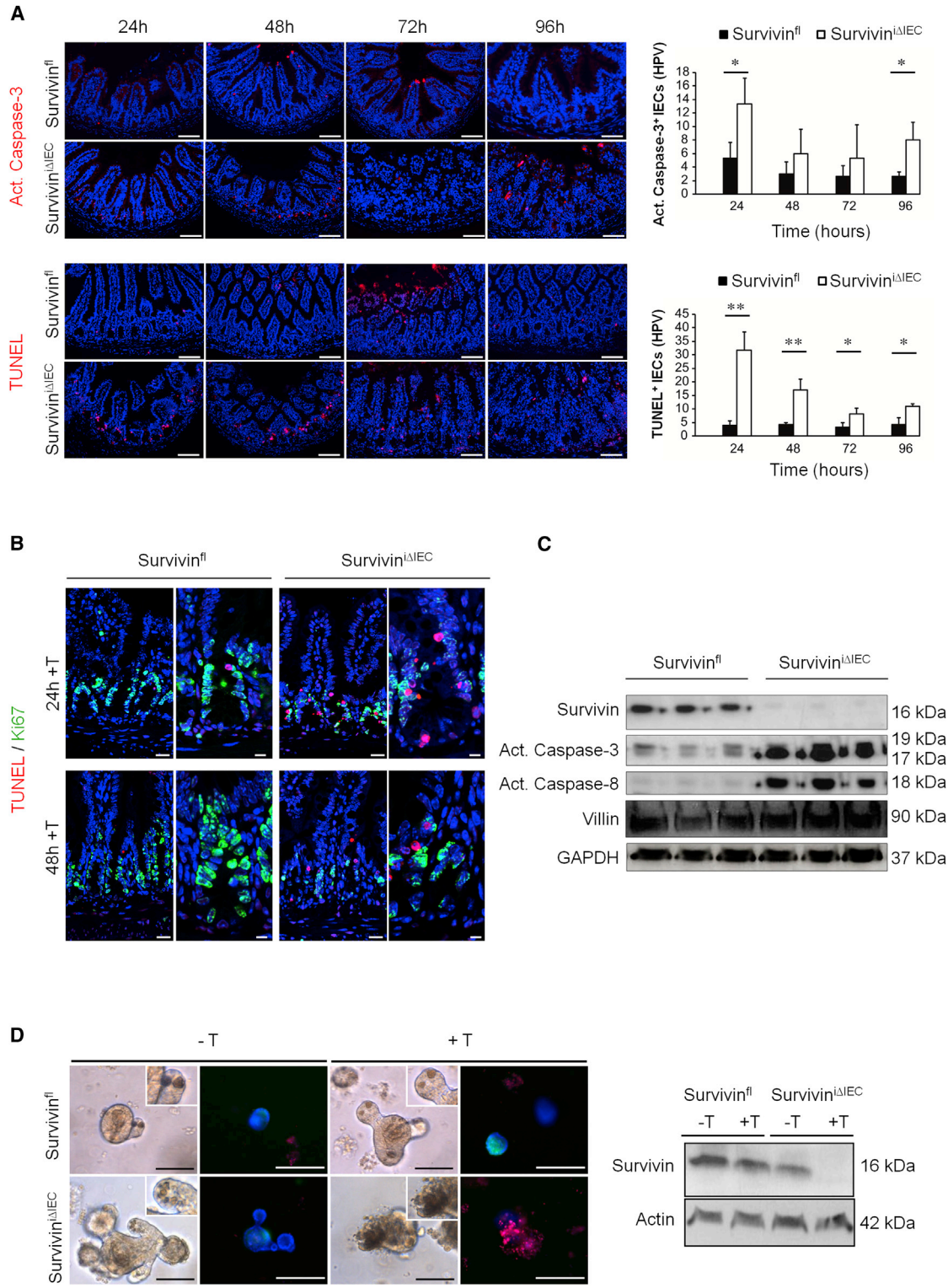

Figure 4. Survivin Deletion Leads to Intestinal Epithelial Cell Death

(A) Left: representative activated caspase-3 (red) and TUNEL (red) stainings of small intestine of Survivin$^{i\Delta IEC}$ and control mice analyzed at indicated time points after starting tamoxifen treatment. Nuclei were stained with Hoechst 33342 (blue). Scale bars, 50 μm. Right: statistics show quantification of activated caspase-3 and TUNEL positive (+) intestinal epithelial cells (IECs) per high-power view (HPV) of Survivin$^{i\Delta IEC}$ and control mice during tamoxifen treatment. Data represent mean values + SD (n = 4 mice per group).

(legend continued on next page)

typical longitudinal nuclei (SCn). In contrast, the appearance of Paneth cells (PCn) was unchanged (Figure 6A). Analysis of subcellular structures within the crypt compartment revealed asymmetric and giant nuclei (Figure 6A, bottom). In fact, the average diameter of these nuclei was almost 3-fold larger after 4 days of tamoxifen treatment in Survivin$^{i\Delta IEC}$ mice than in control mice (Figure 6B). Our findings are in agreement with previous reports on Survivin in other tissues and indicate impaired cell division in epithelial progenitor cells. To get detailed information as to when these nuclear aberrations develop, we analyzed tissue sections via confocal microscopy over time and counted cell divisions in the crypt compartment. We could detect signs of asymmetric cell divisions starting at 24–48 hr after tamoxifen treatment in Survivin$^{i\Delta IEC}$ mice, but not in control mice (Figure 6C). This time point overlapped with the burst of cell death in the crypt compartment which peaked at 48 hr after tamoxifen treatment in Survivin$^{i\Delta IEC}$ mice, supporting the hypothesis that some cells are able to survive but unable to maintain symmetric cell division. Aberrant mitosis as shown by asymmetric and giant nuclei indicates mitotic catastrophe. Survivin is a member of the chromosomal passenger complex and was previously demonstrated to play an important role during cytokinesis in other tissues (Okada et al., 2004; Wu et al., 2009; Hagemann et al., 2013). In fact, we detected a high upregulation of the DNA damage marker γ-H2AX, a hallmark of mitotic catastrophe, in IECs of Survivin$^{i\Delta IEC}$ mice, treated for 72 to 96 hr with tamoxifen (Figure 6D). Furthermore, we found an increased phosphorylation of p53 in Survivin$^{i\Delta IEC}$ mice, which was not detectable in control mice (Figures 6D and S5A). This was supported by western blot analysis, where we show elevated levels of activated caspase-2 in insolated crypt cells of Survivin$^{i\Delta IEC}$ mice (Figure 6E). As a response to DNA damage and the upregulation of phospho-p53, we consequently found upregulated gene expression of p21 and ddit3 after Survivin loss (Figure 6F). Collectively, our data indicate that Survivin is essential for the homeostatic functions of the stem cell compartment. Loss of Survivin expression in epithelial progenitor cells causes mitotic catastrophe and lethal gut tissue degeneration.

DISCUSSION

The importance of Survivin for embryonic development has long been known. However, the role of Survivin in adult tissues appears to be complex and is far less understood (Li and Brattain, 2006). In the present study, we investigated the functional role of Survivin for gut homeostasis using a mouse model of conditional *Survivin* deletion in the intestinal epithelium. The intestinal epithelium is a strong self-regenerating tissue and harbors stem cells and TA cells at the crypt bottom that give rise to all adult differentiated cells of the intestinal epithelium. During the last decade, linage tracing identified markers for cells in the intestinal crypt that showed stem cell potential. Among others, Lgr5 showed a robust stem cell pattern (Barker et al., 2007), and isolated Lgr5^{+} cells were able to build crypt-villus structures in vitro (Sato et al., 2009). Disturbances in the intestinal epithelial homeostasis promote the development of gut-associated diseases such as colorectal cancer and inflammatory bowel disease. Survivin is highly expressed in many tumors, and patients with Survivin overexpressing tumors have a significant lower survival rate (Huang et al., 2013; Zwerts et al., 2007) and a higher risk for metastases (Chu et al., 2012). Our data confirm that Survivin is highly expressed in human as wells as mouse colorectal cancer tissue. However, we also detected Survivin as a constitutively expressed molecule in a subpopulation of epithelial cells residing in the crypt compartment of the intestine.

The crypt compartment is a highly specialized niche where stem cells and TA cells reside and warrant the renewal of the intestinal epithelium. Indeed, we could confirm the expression of Survivin in Lgr5^{+} stem and precursor cells.

Survivin expression in TA cells as well as Lgr5^{+} stem cells is essential as tamoxifen-induced deletion of *Survivin* in intestinal epithelial cells resulted in significant weight loss of mice within few days and abundant inflammation. Disruption of the intestinal tissue architecture could be seen by loss of the villus-crypt structure, finally leading to death of the mice. A functional role of Survivin in Lgr5^{+} cells was directly confirmed by deletion of Survivin specifically in these cells. Excessive caspase activation and cell death could be detected in Lgr5$^{i\Delta Survivin}$ mice as early as 24 hr after tamoxifen application. Of note, Survivin deletion only in Lgr5-expressing stem cells did not lead to changes in gut tissue morphology. This finding is consistent with previous reports depleting Lgr5^{+} cells and has been explained by a functional replacement of Lgr5^{+} stem cells with reserve stem cells, such as Bmi1^{+} stem cells (Tian et al., 2011). Survivin has often been described as a bi-functional protein involved in cell death regulation on the one hand and cell division mechanisms on the other hand. Tissue-specific knockouts of *Survivin* showed different impacts on cellular homeostasis: mice with deletion of *Survivin* in the liver showed no severe phenotype under non-stressed conditions but an increased cell volume and nuclear-DNA content with a reduction of total hepatocyte numbers was observed when compared to controls (Hagemann et al., 2013). In contrast, heart-specific deletion of Survivin led to a premature cardiac death, which was reported to result from a low mitotic rate of cardiomyocytes, but no increase in apoptosis could be detected (Levkau et al., 2008). Similar observations were published for

(B) Confocal microscopy pictures of stainings for TUNEL (red) together with Ki67 (green) in Survivin$^{i\Delta IEC}$ and control mice after 24 and 48 hr (h) of tamoxifen (+T) treatment. Nuclei were counterstained with Hoechst 33342 (blue). Scale bars, 20 μm.

(C) Detection of Survivin and activated caspase-3 and caspase-8 using western blot analysis of isolated intestinal epithelial cell protein lysates of control and Survivin$^{i\Delta IEC}$ mice after 4 days of tamoxifen treatment. Villin and GAPDH were used as internal standard.

(D) Left: light microscopy and fluorescence microscopy pictures of small intestinal organoids from control and Survivin$^{i\Delta IEC}$ mice after 4 days with tamoxifen (+T) and without tamoxifen (−T) treatment. Blue, Hoechst 33342 (cell nuclei); red, propidium iodide (dead cells); green, calcein-AM (viable cells). Scale bars, 200 μm. Right: western blot of protein lysates of organoids from control and Survivin$^{i\Delta IEC}$ mice treated with (+T) or without (−T) tamoxifen for 6 days. Actin was used as internal standard.

See also Figures S2 and S3.

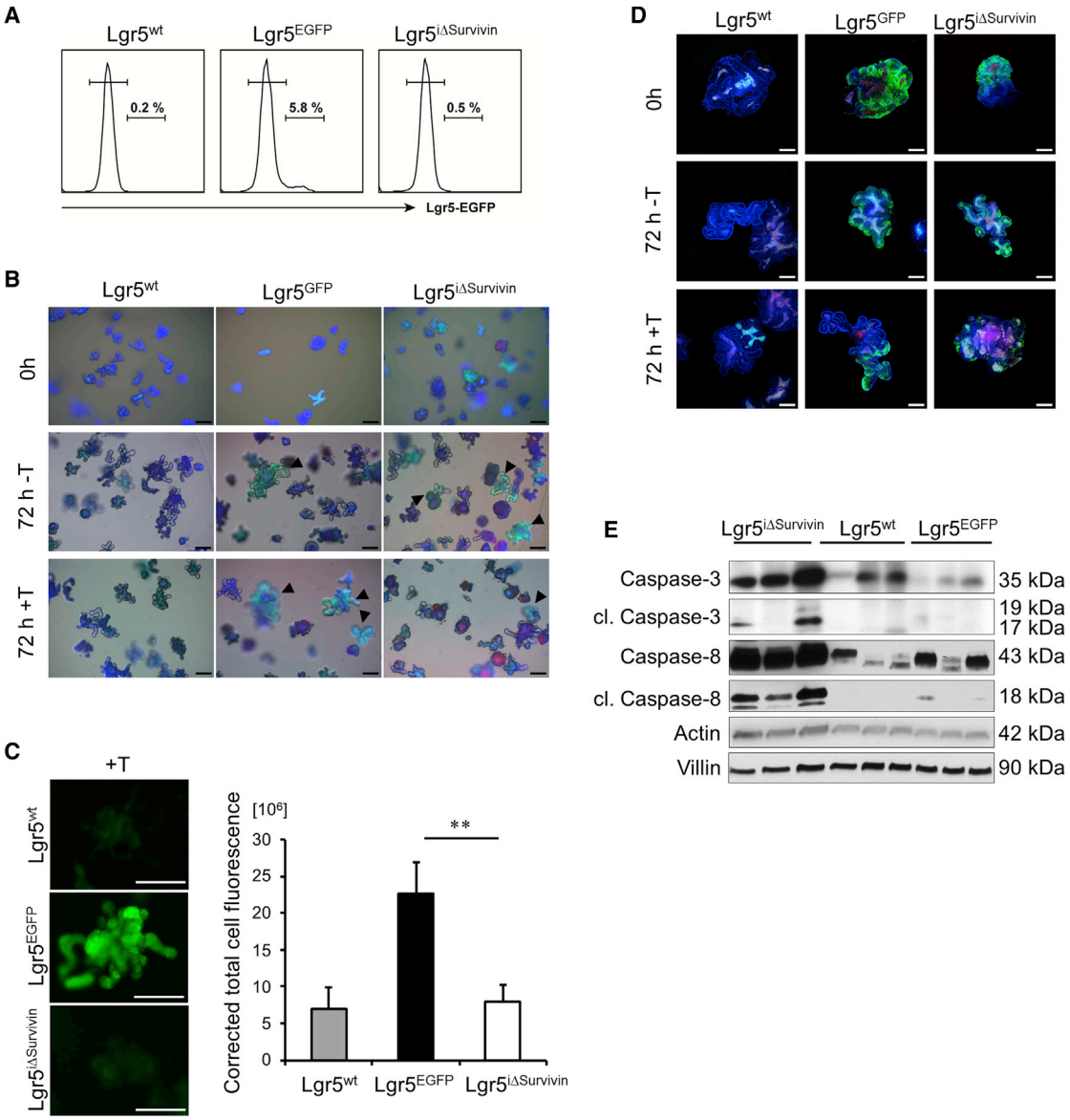

Figure 5. Survivin Is Important for Intestinal Regeneration and LGR5$^+$ Stem Cell Survival

(A) Flow cytometry analysis of expression of Lgr5-EGFP in isolated crypt cells from Lgr5^{wt}, Lgr5^{EGFP}, and Lgr5$^{i\Delta Survivin}$ mice after 3 days of tamoxifen treatment. Gating was performed on EpCam$^+$ (epithelial cells), Survivin$^+$, Zombie-Aqua$^-$ (viable cells) population. Histogram shows EGFP-negative cell population (left peak) and positive cell population (right peak).

(B) Small intestinal organoids from Lgr5^{wt}, Lgr5^{EGFP}, and Lgr5$^{i\Delta Survivin}$ mice grown and additionally treated for 3 days with CHIR99021 and valproic acid, in the steady state (0 hr) and with (+T) or without (−T) tamoxifen treatment for 72 hr (h). Scale bars, 250 μm; blue, Hoechst 33342 (cell nuclei); red, activated caspase-3 (dead cells); green, Lgr5-EGFP. Lgr5^{wt} organoids show autofluorescence (green) of the lumen. Arrows indicate Lgr5-EGFP expressing organoids.

(C) Left: representative fluorescence microscopy pictures of small intestinal organoids derived from Lgr5^{wt}, Lgr5^{EGFP} and Lgr5$^{i\Delta Survivin}$ mice and treated with tamoxifen (+T) for 3 days. Right: corrected mean total cell fluorescence +SD of organoids (n = 9 per group) from Lgr5^{wt}, Lgr5^{EGFP}, and Lgr5$^{i\Delta Survivin}$ mice. Values were calculated using the integrated density, area, and mean fluorescence of the background readings.

(D) Confocal microscopy pictures of organoids from Lgr5^{wt}, Lgr5^{EGFP}, and Lgr5$^{i\Delta Survivin}$ mice grown and additionally treated for 3 days with CHIR99021 and valproic acid, with (+T) and without (−T) tamoxifen treatment for 72 hr (h). Scale bars, 50 μm; blue, Hoechst 33342 (cell nuclei); red, activated caspase-3 (dead cells); green, Lgr5-EGFP. Lgr5^{wt} organoids show autofluorescence (green) of the lumen.

(E) Western blot of protein lysates isolated from intestinal epithelial cells of Lgr5^{wt}, Lgr5^{EGFP}, and Lgr5$^{i\Delta Survivin}$ mice 1 day after tamoxifen injection. Actin and Villin were used as internal controls.

See also Figure S4.

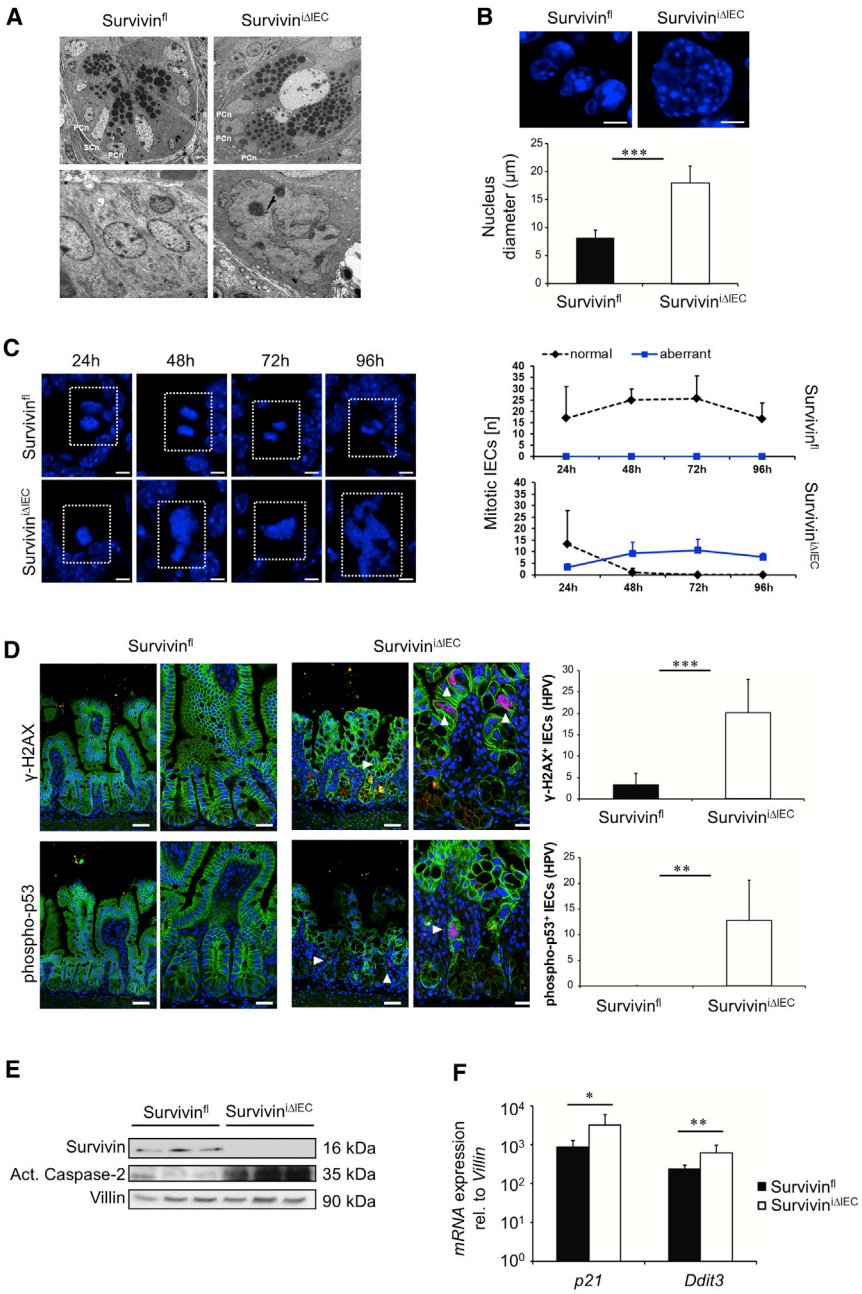

Figure 6. Loss of Survivin Causes Aberrant Mitosis in IECs

(A) Representative electron microscopy pictures of the small intestinal crypt compartment showing Paneth cells with Paneth cell nuclei (PCn) and stem cells with stem cell nuclei (SCn) (top: 2,000× magnification; bottom: 3,150× magnification of IEC cell nuclei) of control and Survivin$^{i\Delta IEC}$ mice after 7 days of tamoxifen treatment.

(B) Representative confocal pictures of IEC nuclei stained with Hoechst 33342 (blue) of the small intestine of control and Survivin$^{i\Delta IEC}$ mice after 4 days of tamoxifen treatment. Statistical analysis showed nuclei almost thrice the size after 4 days of tamoxifen treatment in Survivin$^{i\Delta IEC}$ mice compared to controls. Data represent mean values + SD (n ≥ 4 mice per group). Scale bars, 5 μm.

(C) Left: representative confocal pictures of dividing cells in the crypt compartment of control and Survivin$^{i\Delta IEC}$ mice treated with tamoxifen for indicated time points showing aberrant mitosis. Nuclei were stained with Hoechst 33342 (blue). Scale bars, 5 μm. Boxes show dividing cells within the lower crypt area. Right: time-course analysis of number (n) of IECs during the transition from normal to aberrant mitosis in the crypt compartment of Survivin$^{i\Delta IEC}$ mice compared to controls after starting tamoxifen treatment. Data represent mean values + SD (n = 3 mice per group).

(D) Left: representative fluorescent microscopy pictures showing γ-H2AX (red) and phospho-p53 (red) positive IECs from control and Survivin$^{i\Delta IEC}$ mice together with E-cadherin (green) 4 days after tamoxifen treatment in small intestinal sections. Nuclei were counterstained with Hoechst 33342 (blue). Scale bars, 50 μm; high-power view scale bars, 25 μm. Right: statistical analysis representing γ-H2AX and phospho-p53 positive (+) IECs per high-power view (HPV). Data represent mean values + SD (n ≥ 5 mice per group). Arrows indicate γ-H2AX- and phospho-p53-positive IECs.

(E) Western blot of protein lysates isolated from crypt cells of control and Survivin$^{i\Delta IEC}$ mice after 1 day of tamoxifen treatment detecting Survivin and activated caspase-2. Villin was used as internal standard.

(F) mRNA expression of *p21* and DNA-damage-inducible transcript 3 (*Ddit3*) of small intestinal IECs of Survivin$^{i\Delta IEC}$ mice and control mice relative to *Villin* after 4 days of tamoxifen treatment. Data represent mean values + SD (n ≥ 6 mice per group). See also Figure S5.

the deletion of Survivin in the pancreas. Reduction of the pancreatic beta cell mass was due to a proliferation defect, but increased apoptosis was not involved (Wu et al., 2009). In contrast to the above findings, Survivin expression in the adult intestinal epithelium was found crucial for gut homeostasis and survival. One may speculate that the high need for continuously replenishment in the gut determines the severe phenotype observed in our study.

Moreover, Survivin deletion in IECs was associated with a significant increase in apoptosis. To date, it is not clear if Survivin is able to bind directly to caspases and repress their function (Vercdecia et al., 2000; Shin et al., 2001). In our studies, neither *Caspase-8* or *RIPK3* inhibition nor combined inhibition of both pathways could rescue the severe phenotype of Survivin deficiency. Although we cannot fully exclude an indirect involvement of these pathways at later stages, for example by inflammatory mediators released during tissue damage, our data indicate that neither extrinsic apoptosis nor necroptosis is functionally essential for IEC death following depletion of Survivin. In contrast, our study indicates that mitotic catastrophe is involved in cell death induction upon Survivin deletion, as we observed increased phosphorylation of p53 and H2AX and occurrence of

aberrant cell division. Mitotic catastrophe is debated as a specific form of cell death defined by abnormal mitosis, a physiological mechanism that seems to be important to remove cells with genomic instability and therefore protects from cancer development (Vitale et al., 2011).

The fact that Survivin is mainly expressed during embryogenesis and downregulated in adult tissue has been the rational of using Survivin as a tumor-specific target molecule for anti-cancer therapy. Accordingly, a number of drug candidates aiming at interfering with Survivin expression and function have been developed, such as the transcriptional repressor YM155 (Kelly et al., 2013; Satoh et al., 2009; Tolcher et al., 2008, 2012), antisense oligonucleotides (Talbot et al., 2010), or even vaccines (Tanaka et al., 2013). YM155 is currently investigated in phase 2 trials. Results of this investigation are still pending.

In summary, our findings indicate that Survivin is constitutively expressed in intestinal epithelial progenitor cells in the crypts of Lieberkühn of adult mice and that deletion of Survivin from these cells leads to defects in epithelial homeostasis, destruction of tissue architecture, inflammation, and rapid death. Given our studies, cancer therapies with drugs targeting Survivin in the gut on the one hand could be efficient in eliminating cancer stem cells. However, since our data show that Survivin is essential to preserve gut tissue homeostasis, targeting of Survivin with high efficiency might be associated with a considerable risk for patients treated systemically.

EXPERIMENTAL PROCEDURES

Mice

Mice carrying *loxP*-flanked Survivin alleles (Survivin$^{fl/fl}$) were kindly provided by Hitoshi Okada (Okada et al., 2004). Villin-CreER^{T2} mice were described earlier (el Marjou et al., 2004). Male and female mice were used at an age of 6 to 12 weeks for experiments. Conditional intestinal-epithelium-specific Survivin knockout mice (Survivin$^{i\Delta IEC}$) were generated by breeding Survivin$^{fl/fl}$ mice to Villin-CreER^{T2}-expressing mice. Mice negative for the expression of Villin-CreER^{T2} (Villin-CreER^{T2-}) served as controls in all experiments and are designated Survivin^{fl}. Mice carrying *loxP*-flanked caspase-8 (Beisner et al., 2005) or RIPK3 (Newton et al., 2004) alleles were crossed to inducible Survivin$^{fl/fl}$/Villin-CreER^{T2} mice to generate double-knockout mice (Casp8/Survivin$^{i\Delta IEC}$; RIPK3/Survivin$^{i\Delta IEC}$). The Lgr5-EGFP-IRES-CreER^{T2} mice have been described previously (Barker et al., 2007) and were crossbred to Survivin$^{fl/fl}$ mice to create Lgr5$^{i\Delta Survivin}$ mice. Mice that did not express the transgene (Lgr5^{wt}) and mice that expressed the transgene but did not contain floxed Survivin alleles (Lgr5^{EGFP}) were used as controls for Lgr5$^{i\Delta Survivin}$ mice. To induce CreER^{T2} activity, we used tamoxifen (100 mg/ml dissolved in ethanol; Sigma Aldrich) further diluted in sunflower oil to a concentration of 10 mg/ml. Mice (including controls) were intraperitoneally injected with 100 µl tamoxifen (10 mg/ml) to receive a final tamoxifen dosage of 1 mg each day. For pulse BrdU labeling of cells, mice were intraperitoneally injected with BrdU solution (1 mg; BD Pharmingen) and sacrificed after 4 hr to analyze small intestinal tissue. Mice were examined by measuring weight loss and monitoring of the intestine by high-resolution mouse video endoscopy as previously described (Günther et al., 2011). For endoscopic analysis, mice were anaesthetized by gassing with 2% isoflurane (Abbott) mixed with air.

Animal protocols were approved by the Institutional Animal Care and Use Committee of the University of Erlangen. All mice were kept in individually ventilated cages in compliance with the Animal Welfare Act. Mice were housed at a 12-hr day/night cycle with free access to tap water and food pellets. All mice were kept in mixed cages to avoid cage effects during tamoxifen treatment.

Histology, Immunohistochemistry, and Electron Microscopy

Histological H&E stainings were performed by using formalin-fixed, dehydrated, and paraffin-embedded tissue. Diaminobenzidine staining for Survivin and BrdU was performed by using the ABC staining kit (Santa Cruz) according to the manufacturer's protocol using the following primary antibodies: Survivin (2808, Cell Signaling Technology) and BrdU (ab6326-250 Abcam). Immunofluorescence stainings of cryo- or formalin-fixed, dehydrated, and paraffin-embedded tissue sections were performed using the following primary antibodies: Survivin (2808, Cell Signaling Technology), E-cadherin (MAB7481, R&D Systems), Ki67 (16667, Abcam), activated caspase-3 (9661, Cell Signaling Technology), activated caspase-8 (8592, Cell Signaling Technology), phospho-p53 (9284, Cell Signaling Technology), and γ-H2AX (5438, Cell Signaling Technology). Slides were then incubated with biotinylated secondary antibodies (eBioscience), and signal amplifying was performed using the TSA Cy3 or TSA fluorescein system as recommended by the manufacturer (PerkinElmer) or were incubated by using streptavidin conjugated with Dylight 549 (Jackson ImmunoResearch). Gut tissue from Lgr5-EGFP-IRES-CreER^{T2} mice was fixed in 2% and 4% paraformaldehyde and subsequent incubation in 30% sucrose solution overnight. Double staining for GFP and Survivin was performed by using the anti-GFP antibody conjugated with Alexa 488 (Invitrogen, A21311). Apoptosis was detected by TUNEL staining using an in situ cell death detection kit (Roche). Cell-cycle-sorted intestinal epithelial cells were resuspended in 2% BSA/PBS and centrifuged on BSA-coated glass slides using cytospin (Shandon). Cells were permeabilized by using 0.1% Triton X-100 in PBS for 5 min prior to Survivin staining. Nuclei were counterstained with Hoechst 3342 (Invitrogen). Bright-field microscopy (Leica DMI 4000B), fluorescence microscopy (Leica DMI 4000B), and confocal microscopy (Leica TCS SP5) were used for subsequent analyses. For electron microscopy, glutaraldehyde-fixed tissue was used. After embedding in Epon Araldite, ultrathin sections were cut and analyzed using a Zeiss EM 906.

Intestinal Epithelial Cell Isolation and Western Blotting

IECs were isolated in EDTA/EGTA (Roth) separation buffer as previously described (Nenci et al., 2007). Extraction of proteins was performed on ice by using the mammalian protein extraction buffer (Thermo Scientific) supplemented with protease (EDTA-free) and phosphatase inhibitor tablets (Roche) as well as PMSF (Roche). Proteins were separated by SDS-PAGE using a Mini-Protean-TGX gel (4%–15% polyacrylamide; Bio-Rad) and blotted to a nitrocellulose transfer membrane (Whatman). Membranes were subsequently incubated with the following antibodies: Survivin (2808, Cell Signaling Technology), β-Actin (ab49900, Abcam), glyceraldehyde 3-phosphate dehydrogenase (GAPDH; ab9482, Abcam), activated caspase-2 (ab2251, Abcam), caspase-3 (Cell Signaling Technologies), activated caspase-8 (8592, Cell Signaling Technology), phospho-p53 (Abcam), and Villin (sc-28283, Santa Cruz). As secondary antibody the horseradish peroxidase-linked anti-rabbit antibody (Cell Signaling Technology) was used. Chemiluminescent detection was performed by using an enhanced chemiluminescence substrate (Bio-Rad).

Gene Expression Analysis and Genotyping

Total RNA from IECs and tissue pieces was extracted using the RNA isolation kit (Nucleo Spin RNAII; Macherey Nagel), and cDNA was synthesized by reverse transcription (Script cDNA Synthesis Kit; Jena Bioscience). Real-time PCR was performed with SYBR Green I Master (Roche) and QuantiTect Primer assays (QIAGEN) or gene-specific unmodified DNA oligonucleotides (Eurofins MWG Operon) using the Light Cycler 480 (Roche). Expression signals were normalized to the level of the housekeeping genes hypoxanthine phosphoribosyltransferase (*HPRT*) or *Villin*. Each independent sample was assayed in duplicate.

Genotyping for Survivin was performed by PCR of tail DNA using the primers 5′-TGAGTCGTCTTGGCGGAGGTTGT-3′ and 5′-GCTCGTTCTCGGTAGGGC AGTGG-3′. For determination of IEC-specific knockout of the *Survivin* gene, isolated epithelial cells were used for PCR using the primers 5′-GAGTCC CAGCTTCCAGCGAC-3′ and 5′-CAGGCAAAACCATGCATGTT-3′.

Crypt Isolation, Organoid Culture, and Stainings

For organoid culture, crypts of the small intestine of mice were isolated as previously described (Sato et al., 2009). Organoids of Survivin$^{i\Delta IEC}$ mice

were cultured for at least 5 days and subsequently stimulated with tamoxifen dissolved in ethanol, further diluted in basal culture medium to a final concentration of 50 ng/ml (Sigma Aldrich). As control, organoids were treated with ethanol or DMSO, depending on the dissolvent of the stimuli Organoids derived from $Lgr5^{i\Delta Survivin}$ mice, and controls were treated with CHIR99021 dissolved in distilled water (3 μM; Selleck Chemicals) and valproic acid dissolved in ethanol (1 mM; Biomol) for 3 days before tamoxifen treatment. In some experiments, organoids were treated with a caspase inhibitor (50 μM; Santa Cruz Biotechnology) and/or a pharmacological RIPK3-Inhibitor (5 μM; Calbiochem) or Enbrel (10 μg/ml; Pfizer). Organoid growth was monitored via light microscopy (Leica, DMI 4000B). In vitro analysis of cell death of organoids was performed using the CaspGlow Red Active Caspase Staining kit (Biovision) or Cell Viability kit (Roche) according to the manufacturer's protocol in combination with Hoechst 33342 (Invitrogen). For confocal images, organoids were washed and embedded in Mowiol (Sigma Aldrich).

Flow Cytometry Analysis

Isolation of crypt cells was described previously (Sato et al., 2009). In short, crypts were isolated form fresh small intestine using crypt isolation buffer (PBS + 2 mM EDTA; Roth) and gently rocked for 30 min. at 4°C. To get single cells, isolated crypts were passed through a 70-μm cell strainer (BD Biosciences) and incubated in pre-warmed single-cell dissociation medium made of basal culture medium and Y-27632 (Tocris) for 40–60 min. until crypts started to become loose. Cell suspension was passed through a 40-μm cell strainer (BD Biosciences) followed by a 20-μm cell strainer (Millipore). Single cells were counted and surface-stained using anti-EpCAM antibody (eBioscience) or isotype control using anti-rat immunoglobulin G2a, κ antibody (BioLegend) as well as Zombie-Aqua (BioLegend) and washed twice with FACS washing buffer (PBS + 1% FCS + 10 μM Y-27632). For preservation of GFP bevor intracellular staining, cells were prefixed with 1% PFA for 15 min, and Survivin staining was performed using the FoxP3 Fix/Perm buffer set (BioLegend) after 30-min incubation at 4°C protected from light. Cells were washed twice with permeabilization buffer (eBioscience) followed by incubation with anti-Survivin antibody (Cell signaling Technology) or isotype control using anti-rabbit immunoglobulin G XP (Cell Signaling Technology) for 30 min at 4°C protected from light. Cells were resuspended in 200 μl PBS and analyzed on a LSR Fortessa II (BD Biosciences). Data analysis was performed using FlowJo v7.6.5 (Tree Star). For cell-cycle analysis of intestinal epithelial cells, please see Supplemental Experimental Procedures.

Statistical Analysis

Statistical analysis was performed using the Student's two-tailed t test to compare two groups. Significance levels are indicated as follows: *$p \leq 0.05$, **$p \leq 0.01$, and ***$p \leq 0.001$. Data are presented as mean values + or ± SD. Statistical calculations were performed using standard functions of Microsoft Excel and GraphPad PRISM. Image analysis was performed by ImageJ (NIH), using the integrated density, area of interest, and background readings as parameters. To eliminate bias, investigators were blinded during data collection and data analysis. The block randomization method was used to allocate the animals to experimental group.

SUPPLEMENTAL INFORMATION

Supplemental Information includes Supplemental Experimental Procedures and five figures and can be found with this article online at http://dx.doi.org/10.1016/j.celrep.2016.01.010.

AUTHOR CONTRIBUTIONS

E.M., A.J.W., I.B., N.W., M.L., C.G., M.F.N., and C.B. designed the research. E.M., N.W., E.P., and K.A. performed the experiments. H.O. supplied material that made this study possible. E.M. and C.B. analyzed the data and wrote the paper.

ACKNOWLEDGMENTS

The research leading to these results has received funding from the Interdisciplinary Center for Clinical Research (IZKF) of the University Erlangen-Nuremberg, the European Community's 7th Framework Program (acronym BTCure), and the DFG (SFB796, SFB1181, clinical research unit KFO257, SPP1656). N.W. was further supported by DFG grant BE3686/2.

Received: June 12, 2015
Revised: November 25, 2015
Accepted: December 29, 2015
Published: January 28, 2016

REFERENCES

Altieri, D.C. (2006). Targeted therapy by disabling crossroad signaling networks: the survivin paradigm. Mol. Cancer Ther. *5*, 478–482.

Barker, N., van Es, J.H., Kuipers, J., Kujala, P., van den Born, M., Cozijnsen, M., Haegebarth, A., Korving, J., Begthel, H., Peters, P.J., and Clevers, H. (2007). Identification of stem cells in small intestine and colon by marker gene Lgr5. Nature *449*, 1003–1007.

Barker, N., Bartfeld, S., and Clevers, H. (2010). Tissue-resident adult stem cell populations of rapidly self-renewing organs. Cell Stem Cell *7*, 656–670.

Barker, N., van Oudenaarden, A., and Clevers, H. (2012). Identifying the stem cell of the intestinal crypt: strategies and pitfalls. Cell Stem Cell *11*, 452–460.

Beisner, D.R., Ch'en, I.L., Kolla, R.V., Hoffmann, A., and Hedrick, S.M. (2005). Cutting edge: innate immunity conferred by B cells is regulated by caspase-8. J. Immunol. *175*, 3469–3473.

Boman, B., Kopelovich, L., Siracusa, L.D., Zhang, T., Henderson, K., Cofer, Z., Buchberg, A.M., Fields, J.Z., and Otevrel, T. (2009). A Tcf4-GFP reporter mouse model for monitoring effects of Apc mutations during intestinal tumorigenesis. Mol. Carcinog. *48*, 821–831.

Chu, X.-Y., Chen, L.-B., Wang, J.-H., Su, Q.-S., Yang, J.-R., Lin, Y., Xue, L.-J., Liu, X.B., and Mo, X.B. (2012). Overexpression of survivin is correlated with increased invasion and metastasis of colorectal cancer. J. Surg. Oncol. *105*, 520–528.

Conway, E.M., Pollefeyt, S., Steiner-Mosonyi, M., Luo, W., Devriese, A., Lupu, F., Bono, F., Leducq, N., Dol, F., Schaeffer, P., et al. (2002). Deficiency of survivin in transgenic mice exacerbates Fas-induced apoptosis via mitochondrial pathways. Gastroenterology *123*, 619–631.

el Marjou, F., Janssen, K.-P., Chang, B.H.-J., Li, M., Hindie, V., Chan, L., Louvard, D., Chambon, P., Metzger, D., and Robine, S. (2004). Tissue-specific and inducible Cre-mediated recombination in the gut epithelium. Genesis *39*, 186–193.

Fukuda, S., and Pelus, L.M. (2006). Survivin, a cancer target with an emerging role in normal adult tissues. Mol. Cancer Ther. *5*, 1087–1098.

Günther, C., Martini, E., Wittkopf, N., Amann, K., Weigmann, B., Neumann, H., Waldner, M.J., Hedrick, S.M., Tenzer, S., Neurath, M.F., and Becker, C. (2011). Caspase-8 regulates TNF-α-induced epithelial necroptosis and terminal ileitis. Nature *477*, 335–339.

Hagemann, S., Wohlschlaeger, J., Bertram, S., Levkau, B., Musacchio, A., Conway, E.M., Moellmann, D., et al. (2013). Loss of Survivin influences liver regeneration and is associated with impaired Aurora B function. Cell Death Differ. *20*, 834–844.

Huang, Y.-J., Qi, W.-X., He, A.-N., Sun, Y.-J., Shen, Z., and Yao, Y. (2013). The prognostic value of survivin expression in patients with colorectal carcinoma: a meta-analysis. Jpn. J. Clin. Oncol. *43*, 988–995.

Jiang, Y., de Bruin, A., Caldas, H., Fangusaro, J., Hayes, J., Conway, E.M., Robinson, M.L., and Altura, R.A. (2005). Essential role for survivin in early brain development. J. Neurosci. *25*, 6962–6970.

Kelly, R.J., Thomas, A., Rajan, A., Chun, G., Lopez-Chavez, A., Szabo, E., Spencer, S., et al. (2013). A phase I/II study of sepantronium bromide (YM155, Survivin suppressor) with paclitaxel and carboplatin in patients with advanced non-small-cell lung cancer. Ann. Oncol. *24*, 2601–2606.

Levkau, B., Schäfers, M., Wohlschlaeger, J., von Wnuck Lipinski, K., Keul, P., Hermann, S., Kawaguchi, N., Kirchhof, P., Fabritz, L., Stypmann, J., et al. (2008). Survivin determines cardiac function by controlling total cardiomyocyte number. Circulation *117*, 1583–1593.

Li, F., and Brattain, M.G. (2006). Role of the Survivin gene in pathophysiology. Am. J. Pathol. *169*, 1–11.

Miura, K., Fujibuchi, W., Ishida, K., Naitoh, T., Ogawa, H., Ando, T., Yazaki, N., Watanabe, K., Haneda, S., Shibata, C., and Sasaki, I. (2011). Inhibitor of apoptosis protein family as diagnostic markers and therapeutic targets of colorectal cancer. Surg. Today *41*, 175–182.

Mobahat, M., Narendran, A., and Riabowol, K. (2014). Survivin as a preferential target for cancer therapy. Int. J. Mol. Sci. *15*, 2494–2516.

Nenci, A., Becker, C., Wullaert, A., Gareus, R., van Loo, G., Danese, S., Huth, M., Nikolaev, A., Neufert, C., Madison, B., et al. (2007). Epithelial NEMO links innate immunity to chronic intestinal inflammation. Nature *446*, 557–561.

Newton, K., Sun, X., and Dixit, V.M. (2004). Kinase RIP3 is dispensable for normal NF-kappa Bs, signaling by the B-cell and T-cell receptors, tumor necrosis factor receptor 1, and Toll-like receptors 2 and 4. Mol. Cell. Biol. *24*, 1464–1469.

Okada, H., Bakal, C., Shahinian, A., Elia, A., Wakeham, A., Suh, W.-K., Duncan, G.S., Ciofani, M., Rottapel, R., Zúñiga-Pflücker, J.C., and Mak, T.W. (2004). Survivin loss in thymocytes triggers p53-mediated growth arrest and p53-independent cell death. J. Exp. Med. *199*, 399–410.

Sancho, E., Batlle, E., and Clevers, H. (2003). Live and let die in the intestinal epithelium. Curr. Opin. Cell Biol. *15*, 763–770.

Sato, T., Vries, R.G., Snippert, H.J., van de Wetering, M., Barker, N., Stange, D.E., van Es, J.H., et al. (2009). Single Lgr5 stem cells build crypt-villus structures in vitro without a mesenchymal niche. Nature *459*, 262–265.

Satoh, T., Okamoto, I., Miyazaki, M., Morinaga, R., Tsuya, A., Hasegawa, Y., Terashima, M., Ueda, S., Fukuoka, M., Ariyoshi, Y., et al. (2009). Phase I study of YM155, a novel survivin suppressant, in patients with advanced solid tumors. Clin. Cancer Res. *15*, 3872–3880.

Shin, S., Sung, B.J., Cho, Y.S., Kim, H.J., Ha, N.C., Hwang, J.I., Chung, C.W., Jung, Y.K., and Oh, B.H. (2001). An anti-apoptotic protein human survivin is a direct inhibitor of caspase-3 and -7. Biochemistry *40*, 1117–1123.

Talbot, D.C., Ranson, M., Davies, J., Lahn, M., Callies, S., André, V., Kadam, S., Burgess, M., Slapak, C., Olsen, A.L., et al. (2010). Tumor Survivin is down-regulated by the antisense oligonucleotide LY2181308: a proof-of-concept, first-in-human dose study. Clin. Cancer Res. *16*, 6150–6158.

Tanaka, T., Kitamura, H., Inoue, R., Nishida, S., Takahashi-Takaya, A., Kawami, S., Torigoe, T., Hirohashi, Y., Tsukamoto, T., Sato, N., and Masumori, N. (2013). Potential survival benefit of anti-apoptosis protein: survivin-derived peptide vaccine with and without interferon alpha therapy for patients with advanced or recurrent urothelial cancer–results from phase I clinical trials. Clin. Dev. Immunol. *2013*, 262967.

Tian, H., Biehs, B., Warming, S., Leong, K.G., Rangell, L., Klein, O.D., and de Sauvage, F.J. (2011). A reserve stem cell population in small intestine renders Lgr5-positive cells dispensable. Nature *478*, 255–259.

Tolcher, A.W., Mita, A., Lewis, L.D., Garrett, C.R., Till, E., Daud, A.I., Patnaik, A., Papadopoulos, K., Takimoto, C., Bartels, P., et al. (2008). Phase I and pharmacokinetic study of YM155, a small-molecule inhibitor of survivin. J. Clin. Oncol. *26*, 5198–5203.

Tolcher, A.W., Quinn, D.I., Ferrari, A., Ahmann, F., Giaccone, G., Drake, T., Keating, A., and de Bono, J.S. (2012). A phase II study of YM155, a novel small-molecule suppressor of survivin, in castration-resistant taxane-pretreated prostate cancer. Ann. Oncol. *23*, 968–973.

Uren, A.G., Wong, L., Pakusch, M., Fowler, K.J., Burrows, F.J., Vaux, D.L., and Choo, K.H. (2000). Survivin and the inner centromere protein INCENP show similar cell-cycle localization and gene knockout phenotype. Curr. Biol. *10*, 1319–1328.

van de Wetering, M., Sancho, E., Verweij, C., de Lau, W., Oving, I., Hurlstone, A., van der Horn, K., Batlle, E., Coudreuse, D., Haramis, A.P., et al. (2002). The beta-catenin/TCF-4 complex imposes a crypt progenitor phenotype on colorectal cancer cells. Cell *111*, 241–250.

Verdecia, M.A., Huang, H., Dutil, E., Kaiser, D.A., Hunter, T., and Noel, J.P. (2000). Structure of the human anti-apoptotic protein survivin reveals a dimeric arrangement. Nat. Struct. Biol. *7*, 602–608.

Vitale, I., Galluzzi, L., Castedo, M., and Kroemer, G. (2011). Mitotic catastrophe: a mechanism for avoiding genomic instability. Nat. Rev. Mol. Cell Biol. *12*, 385–392.

Wu, X., Wang, L., Schroer, S., Choi, D., Chen, P., Okada, H., and Woo, M. (2009). Perinatal survivin is essential for the establishment of pancreatic beta cell mass in mice. Diabetologia *52*, 2130–2141.

Yin, X., Farin, H.F., van Es, J.H., Clevers, H., Langer, R., and Karp, J.M. (2014). Niche-independent high-purity cultures of Lgr5+ intestinal stem cells and their progeny. Nat. Methods *11*, 106–112.

Zwerts, F., Lupu, F., De Vriese, A., Pollefeyt, S., Moons, L., Altura, R.A., Jiang, Y., Maxwell, P.H., Hill, P., Oh, H., et al. (2007). Lack of endothelial cell survivin causes embryonic defects in angiogenesis, cardiogenesis, and neural tube closure. Blood *109*, 4742–4752.